Anti-Corrosion Behaviour of Silver-Cobalt Oxide-Titanium Dioxide Nanocomposites Coated Mild Steel in Sea water

*[1]Mohammed Ibrahim,[2]Joseph B. Agboola, [3,5]Ambali S. Abdulkareem, [1]Oyewole Adedipe, and [4,5]Jimoh O. Tijani
[1]Department of Mechanical Engineering, Federal University of Technology, Minna, Nigeria
[2]Department of Materials and Metallurgical Engineering, University of Lagos, Akoka, Nigeria
[3]Department of Chemical Engineering, Federal University of Technology, Minna, Nigeria
[4]Department of Chemistry, Federal University of Technology, Minna, Nigeria
[5]Centre for Biotechnology and Genetic Engineering, Federal University of Technology, Minna, Nigeria
abuhannatu@yahoo.com | joeagboola@gmail.com | {kasaka2003 | oye.adedipe | jomohtijani}@futminna.edu.ng

Received: 14-JUL-2020; Reviewed: 16-AUG-2020; Accepted: 26-AUG-2020
http://dx.doi.org/10.46792/fuoyejet.v5i2.549

Abstract- The research work investigates the corrosion resistance of Silver-Cobalt Oxide-Titanium Dioxode ($Ag/Co_3O_4/TiO_2$) nanocomposites coated mild steel (AISI 1020) in seawater environment. The coatings were carried out by dipping method. The nanoparticles were individually produced by mixing the salt precursors with extract of *Piptadeniastrum africana* leaf under the optimized synthesis conditions. The $Ag/Co_3O_4/TiO_2$ nanocomposite was produced by mixing Ag, Co_3O_4 and TiO_2 NPs in equal proportions to constitute 75 wt% of the composite. 10 wt % epoxy resin and its hardener in the ratio (1:1) were added to serve as the binder, while 15 wt% of CNT was introduced to serve as support. Phase and Microstructural examination of the coatings was carried out by XRD and HRSEM. The corrosion protection properties were determined by using computer- controlled EGG 273A Potentiostat with three- electrode cell system under static laboratory conditions using the linear potentio-dynamic polarization method. The coated sample was dried at temperatures of 100°C to enhance adherence of the coating on the steel substrate. The result of Tafel polarization plots revealed improved corrosion resistance of the coated specimen as compared to as-received sample. Corrosion rate and corrosion resistance of 0.201 m/y and 195.12 Ω were recorded against the coated sample while 0.261 m/y and 71.42 Ω were recorded for the as-received sample respectively. The coated sample exhibited higher potential shift in the positive direction and showed better corrosion resistance properties.

Keywords- Nanocomposite, Mild steel, Corrosion, Potentio-Dynamic polarization, Seawater

1 INTRODUCTION

The use of mild steel (AISI 1020) is indispensable in all endeavours of life. Seidu and Kutelu, (2013) revealed that mild steel accounts for over 98% of the construction materials due to its excellent mechanical properties. Also, Umeozokwere *et al.,* (2016) highlighted that mild steel is of low cost as compared to other fabrication metals. However, the problem with mild steel is that it easily corrodes particularly in aggressive environment such as seawater. Failures in mild steel structures due to corrosion attacks are very expensive in terms of waste of resources and loss of human lives.

According to Umoru, (2001), in developed countries like United States of America (USA), it was estimated that cumulative costs resulting from corrosion annually is about 300 Million USD and in developing countries such as Nigeria, it was estimated to be about 10 Million USD. Somayeh, *et al.,* (2018) pointed out that among the methods available for corrosion prevention, coating method is considered one of the most effective method. Although several metals and nonmetals, ceramics and polymer materials were used for coating of steel to enhance surface hardness, wear, fatigue and corrosion resistant, certain limitations are eminent depending on application and service conditions. Muhammad, (2012), found out that coatings from organic sources like epoxy coatings can breakdown under excessive temperature, these may result to delamination, pore formation blisters and cracking which affect the corrosion protection properties. Several authors have reported successful application of nano-coatings to mitigate corrosion.

Srivastava *et al.,* (2013), studied electro deposition of Ni-Cr_2O_3 nanocomposites and showed that the application of these nanocomposites coated on steel surface improved the tribological and mechanical properties of the steel. Malatji and Popoola, (2015) fund that ternary coating from $Zn/Cr_2O_3/SiO_2$ deposited on steel using electrolytic chloride bath solution showed improvement in tribological behaviour and better thermal stability under aggressive corrosion environment.

Furthermore, Fayomi and Popoola (2013), discovered that there was improved corrosion resistance of mild steel coated with Zn- Co - TiO_2 nanocomposite. It was reported that the improved interfacial interaction between the nanoparticles and the specimen led to improved corrosion resistance. Despite the wonderful performance of metal and metal oxide nanoparticles, the major problems associated with the nanoparticles coatings is the particle agglomeration which often creates voids and coating cracks which consequently lead to poor adhesion between the coating interface and the substrates. Routes are created through which corrosion is initiated and propagated. In this research study, nanocomposite coatings from nanoparticles of silver, cobalt oxide and titanium-dioxide synthesized by greens method was produced and applied on mild steel substrates. The nanocomposite was characterized by HRSEM and XRD analysis. Reduction in particle agglomeration and improvement in coating adhesion at substrate/coating interface were achieved. These in turn reduced the cracks and voids tendencies of the nanoparticles coating and consequently resulted to better corrosion protection of the coated specimen in the medium.

*Corresponding Author

2 MATERIAL/EQUIPMENT

The specimen utilized in this work was obtained from scrap market in Minna, Niger State, Nigeria. Chemicals and reagents were obtained from Sigma Aldrich, China and Kamel, England. They include, silver nitrate($AgNO_3$) at 99.8% purity, cobalt (II) nitrate, $Co(NO_3)_2.6H_2O$, (97%), titanium (IV) isopropoxide (97%), carbon nanotube (CNT) (95%), concentrated hydrochloric acid (HCl) (90%), sodium hydroxide (NaOH) (90%), distilled water (95%), acetone (97%), aluminium chloride (95%), sodium acetate, sodium carbonate (Na_2CO_3), (95%), 10% Folin-Ciocalteau's reagent (95%), silver, cobalt oxide and titanium dioxide nanoparticles. Other equipment used include; Emery papers of 220, 400, 600 and 800 grits, magnetic stirrer, freeze drier, ultrasonic bath, high speed refrigerated centrifuge, high resolution SEM.

2.1 PREPARATION OF SAMPLES

2.1.1 Mild steel

AISI 1020 mild steel rod of 10 mm diameter was used for this work. Ten (10) samples were cut for the corrosion test according to American Society for Testing and Materials standard, ASTM – G59-97 (2009), Eight (8) of the samples were normalized by heating in muffle furnace to austenitic temperature of 850^{o}C and held for 30 mins. and thereafter cooled in still air to relieve the samples of machining stress, followed by grinding with emery papers of 220, 400, 600 and 800 grits, washed with distilled and degreased in acetone. (Abdulrahman, *et al.,* 2017). Two (2) of the samples were designated as "As-received" samples.

2.1.2 Synthesis of Ag, Co_3O_4 and TiO_2 Nanoparticles

Piptadeniastrum africana leaf extract were utilized for the reduction of metals to nanoparticles. 10g of dried leaves powder were boiled in 100ml of distilled water for 15min. at 60^{o}C. The extract was obtained by filtration method using Whatman No.42 filter paper. The phytochemical analysis carried out on the representative extract sample showed a high phenolic content of 4 mg/g and it is therefore used for the synthesis of the nanoparticles. Ag nanoparticles was produced using the method described by Krishnaraj, *et al.,* (2014). A mixture of 1 ml of the extract and 10 ml of aqueous $AgNO_3$ under a pH of 8 at 35^{o}C for 60 minutes. Cobalt Oxide nanoparticles were synthesized using the method described by Koyyoti, *et al.,* (2016). A mixture of 10 ml of the extract and 50 ml of $1x10^{-3}$M aqueous $Co(NO_3)_2.6H_2O$ solution at an incubation temperature of 40^{o}C for 60 minutes. The TiO_2 particles were synthesized following Sundararajan and Gowri, (2011). 20 ml of distilled water were added to 20 ml of aqueous leaf extract in an Erlenmeyer flask under continuous stirring condition using magnetic stirrer and then 10 ml of aqueous titanium tetra-iso-propoxide solution was added drop wisely. The mixture was kept under continuous stirring at room temperature for two (2) hours. The formed TiO_2 nanoparticles were acquired by washing severally with distilled water. The colloidal TiO_2 nanoparticles were oven dried at 100^{o}C for two hours and calcined at 450^{o}C for further two hours in a muffle furnace.

2.1.3 Production of Carbon Nanotube (CNT)

Carbon nanotubes were produced following the method described by Abdulrahman, *et al.,* (2017). 1 g of calcined Fe-Ni alloy catalyst was measured in ceramic quartz boot using weighing balance, the weight of the catalyst and the quartz boot was recorded, the quartz boot was inserted in the furnace tube and was adjusted to the Centre of the reaction chamber of the CVD equipment. The CVD equipment was programmed to heat at 10^{0}C per minute to the temperature of 750^{0}C. The Argon which served as the carrier gas for the carbon source (ethylene) was initially set to flow at 30ml/min. to purge the furnace as the temperature rises to 750^{0}C. This was done to flush all impurity gases that could affect the catalytic activities in the tube. As the temperature reached 750^{0}C, the flow rate of the Argon was increased to 230ml/min. and the carbon source (ethylene) which was initially programmed to flow at 200ml/min. was introduced. According to the CVD inputted program, the furnace was set to hold at 750^{0}C for 60 mins. After the process, the CVD was allowed to cool to ambient temperature, the quartz boot with the produced CNTs were collected and weighed to evaluate the percentage yield of the CNTs. The CNTs appeared in form of clump, which was gently ground to particles using ceramic mortar and pestle.

2.1.4 Preparation of Silver/Cobalt Oxide/Titanium Dioxide ($Ag/Co_3O_4/TiO_2$) Nanocomposite Using CNT as Support

$Ag/Co_3O_4/TiO_2$ nanocomposite was produced by mixing Ag, Co_3O_4 and TiO_2 nanoparticles in equal proportion which add up to 75 wt% of the composite. 10 wt % of epoxy resin and its hardener in the ratio (1:1) were added to serve as the binder, while 15 wt% of CNT was introduced to serve as support. The mixture was stirred at a speed of 1200 rpm for 15 mins. using magnetic stirrer and sonicated in acetone for another 15 mins. using ultrasonic bath. 5 % of the binder and the mixture were further stirred and sonicated for further 15 mins. Finally, 5% epoxy hardener were added and the resulting mixture were stirred for another 10 mins.

2.2 CHARACTERIZATION OF MILD STEEL AND SEAWATER SAMPLES

The sample of the obtained mild steel was characterized using Spectro MIDEX-MID05 X-Ray Energy Fluorescence Spectrometer metal analyser for chemical composition, while the sample of seawater obtained from Lagos lagoon was characterized by chromatographic methods. In other to examine the morphology of mild steel samples before and after corrosion, High Resolution Scanning Electron Microscopy (HRSEM), Magellan 400L, was utilized for analysis.

2.3 POTENTIO-DYNAMIC POLARIZATION TEST

The potentio-dynamic polarization measurements were carried out in line with the procedures described by Abdulrahman, *et al.,* (2017). The setup consists of computer- controlled EGG 273A Potentiostat with three-electrode cell system. The test was conducted under static laboratory conditions. The corrosion cell consists a saturated calomel electrode (SCE) as reference, platinum

http://dx.doi.org/10.46792/fuoyejet.v5i2.549 engineering.fuoye.edu.ng/journal

grid as the counter electrode and specimen as working electrode (WE). The potential (E) of the working electrode were maintained within the range of ± 2.5V at a scanning rate of 5mVs^{-1}. The WE was dipped in the corrosion medium for 15 mins. this established the open circuit potential (OCP) and other measurements were taken within the potential range. All electrochemical tests were performed at 35^{o}C. The rate of corrosion was calculated using ASTM relation in equations (1) as suggested by (Shetty and Shetty, 2016).

$$Corrosion\ Rate\ (CR)Mpy = \frac{0.129\ X\ M\ X\ Icorr}{D} \quad (1)$$

Where *CR* is the Corrosion rate Mpy
M represents the molecular weight of the steel sample.
I_{corr} represents the corrosion current density (I Am^{-2})
D represents the density of the steel = 7870kg/m^3. (amesweb.info/Materials/Density_of_steel.aspx)

The polarization resistance was obtained from Stean Gary equation as shown in Equation 2 (Shetty and Shetty, 2016).

$$Rp = \frac{\beta a \beta c}{2.303(\beta a + \beta c)Icorr} \quad (2)$$

Where β_a and β_c (Vdec^{-1}) represents the Tafel polarization constants which were derived from the anodic and cathodic slopes.

3 Results / Discussion

3.1 Characterization of Mild Steel and Seawater

The composition of the metallic substrate is shown in Table1. It consists of 0.23wt% carbon, 0.43 wt% manganese, 0.035 wt% phosphorous, 0.025 wt% sulphur and 99.09 wt% iron. These by the American Iron and Steel Institute (AISI), represents AISI 1020 steel (http://www.azom.com/article.aspx. ID 6114).

Table 1. Chemical composition of control Sample

Elements	%Composition
C	0.23
Si	0.038
S	0.025
P	0.035
Mn	0.43
Ni	0.011
Cr	0.012
Mo	0.012
V	0.002
Cu	0.004
W	0.001
As	0.03
Sn	0.02
Co	0.02
Al	0.01
Zn	0.03
Fe	99.09

3.1.1 Chemical composition of Seawater

Table 2 shows the chemical composition of the sampled seawater.

Table 2. Physicochemical screening of Seawater sample

Parameter	Unit	Value
Temperature °C		28.35
Turbidity	NTU	20.50
pH		7.4
Conductivity	μΩ/cm	60754
TSS	mg/l	4783.00
Alkalinity	"	43.25
Acidity	"	15.60
Total hardness	"	314.20
DO	"	5.50
BOD	"	7.50
COD	"	135.0
Cl^-	"	314.0
Sulphate	"	80.0
Nitrate	"	80.70
TDS	"	841.20

Dissolved oxygen (DO), pH, temperature, salinity and sulphate are some of the major parameters that influence the rate of corrosion in seawater medium. Barchiche, *et al.*, (2009) found that presence of Cl^- in seawater leads to increase corrosion rate. Cl- enhances breakdown of passive layers of the formed oxides which often leads to local, crevice or pit corrosions. The value of 314 mg/l shown in Table 2 is high to cause acceleration of the breaking down of the passive layer to aggravates corrosion. Acid corrosion is most prevalent at low pH values, similarly the rate of corrosion is high at high pH values due to caustic embrittlement. Therefore, the value of 7.4 recorded in this case is responsible for the increase in the rate of corrosion of the specimen in this medium. The presence of sulphate ions enhances the formation of calcium and magnesium deposits that impedes the rate of corrosion (Sundjono, *et al.*, 2017). At pH of 7.4, this may have gone into solution and consequently increased the rate of corrosion. Dissolved oxygen and temperature have proportionate increase on the corrosion rate. Temperature aggravates diffusion rate of metallic ions and consequently promote depolarization and water conductivity hence corrosion rate is increased. Similarly, DO increases rate of corrosion due to increased rate of cathodic reaction. It was noticed from Table 2 that the values of 28.35^{o}C and 5.50 mg/l for temperature and DO respectively are high and responsible for increase rate of corrosion in this medium. Sundjono, *et al.*, (2017), pointed out that water salinity has remarkable influence on water resistivity.

3.2 Characterization of Ag/Co3O4/TiO2 Nanocomposite

3.2.1 SEM Micrographs of Ag, Co_3O_4, TiO_2 Nanoparticles and Ag/Co_3O_4/TiO_2Nanocomposite

The SEM micrographs of silver, Cobalt Oxide Titanium dioxide nanoparticle and Purified Carbon nanotubes CNTs are shown in plate 1.

http://dx.doi.org/10.46792/fuoyejet.v5i2.549 engineering.fuoye.edu.ng/journal

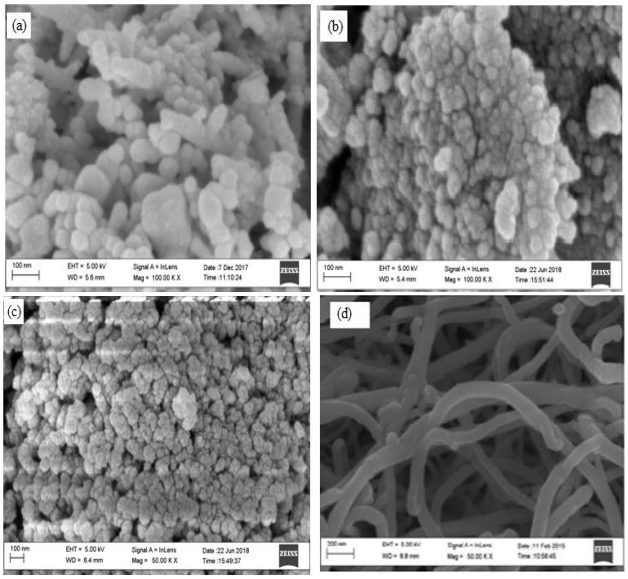

Plate 1: SEM Micrographs of (a) Silver NPs, (b) Cobalt Oxide NPs, (c) Titanium dioxide NPs and (d) Purified Carbon Nanotubes CNTs

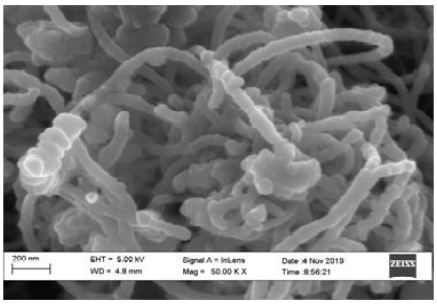

Plate 2: SEM Micrographs of $Ag/Co_3O_4/TiO_2$ nanocomposite

The SEM micrograph of individual components of the composite is shown in plate 1 (a), (b), (c) and (d). While that of composite is shown in plate 2. It can be observed from plate II that other elements in the composite are embedded in the carbon nanotubes as indicated by the white and dark spots. The CNT was able to accommodate other elements due to its large surface to area ratio.

3.2.2 XRD Characterization of $Ag/Co_3O_4/TiO_2$ Nanocomposite

The XRD pattern of $Ag/Co_3O_4/TiO_2$ nanocomposite is shown in Figure 1.

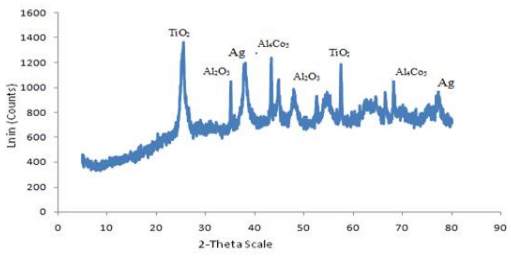

Fig. 1: XRD pattern of $Ag/Co_3O_4/TiO_2$ Nanocomposite

The elemental composition of the composite was detected by XRD analysis as shown in Figure 1. TiO_2 was detected at 25.4° corresponding to (101) and at 57.3° corresponding to (211) planes in hexagonal packed structure. Ag was detected at 38.2° corresponding to (101) and 78.6° corresponding to (301) planes in fcc structure. Al_2O_3 was detected at 35.1° while cobalt existed in form of $AlCo_3$ at 41.0° and 68.3°. The presence of aluminium in the form of $Al_2O_3$and $AlCo_3$ were attributed to instrumental impurities. This shows that the composite was consisted of the three elements expected to form the composite.

3.3 Corrosion Test for Ag/ Co_3O_4/ TiO_2 Nanocomposite Coated Mild Steel Samples in Seawater.

Figure 2 show the Tafel polarization curves for as-received and coated samples.

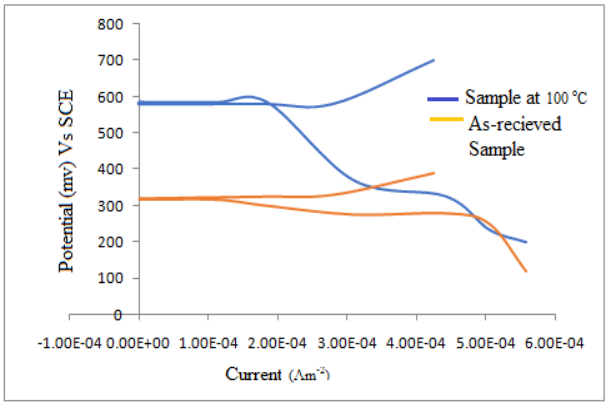

Fig. 2: Tafel polarization plots for control and coated samples in seawater environment

Parameters such as current density (I_{corr}), Corrosion potential (E_{corr}), corrosion rate (CR), anodic and cathodic slopes (β_a and β_c) were obtained from the Tafel plots in Figure 2 as shown below in Table 3.

Table 3. Electrochemical Corrosion Parameters for As-Received and Coated Samples

Sample ID	I_{corr} (mAm^{-2})	Ecorr (mV)	β_a (V/ dec)	β_c (V/ dec)	Corr Rate (m/y)	Corr Resist (Ω)
As-received	0.285	317.4	75	125	0.261	71.42
Coated Sample	0.220	510.2	150	290	0.201	195.12

From the polarization curves in Figure 2, significant shift towards the positive potential were noticed. according to Atta, *et al.*, (2014) the shift represents improvement in corrosion resistance due to the coating on the sample. The extrapolation of the linear portion of the Tafel region in either the cathodic or anodic polarization curve to potential (E_{corr}) gives the current density (I_{corr}) which was used in evaluating corrosion rate as well as corrosion resistance from equations 1 and 2 respectively. The corrosion rates and the corrosion resistances obtained for the as-received and the coated sample are 0.261 m/y, 71.42Ω and 0.201 m/y, 195.12Ω respectively. It is therefore evident that the coated sample has shown remarkable improvement in suppressing corrosion in seawater environment as compared to as-received sample. The curing of the coating at a temperature of 100°C improved adhesion at substrate/coating interface and reduced the particle agglomeration which in turn reduced the cracks

http://dx.doi.org/10.46792/fuoyejet.v5i2.549 engineering.fuoye.edu.ng/journal

and voids tendencies of nanoparticle coating and consequently reduced the corrosion rate. The indication of better corrosion performance by the positive shift in corrosion potential exhibited in this study is in-line with the work of Malatji and Popoola, (2015), the authors studied electrodeposition of ternary Zn-CrO3-SiO2 nanocomposite coating on mild steel for extended applications and also that of Fayomi and Popoola (2013), who studied the anti-corrosion properties and structural characteristics of Zn–Co–TiO2 coatings on mild steel substrate.

3.4. Microstructural Examination of the Steel Samples

3.4.1 As-received Sample

Plate 3 show the high-resolution scanning electron microscope cross- section images of as-received sample before and after corrosion in seawater environment.

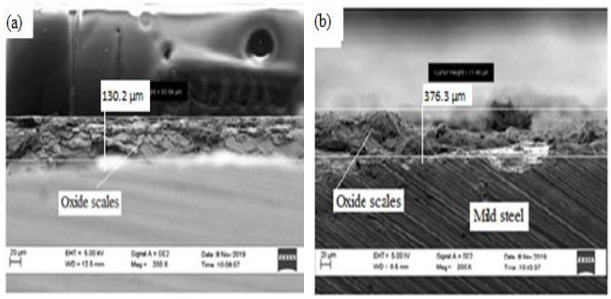

Plate 3: SEM cross-sectional view of as-received mild steel sample (a) prior to corrosion test (b) After corrosion test

The image of Plate 3 (a) revealed the presence of single layer of 130.2 µm thick, compact and crystalline rust products. The corrosion scales observed on plate 3 (a) was due to interaction of mild steel with the environment which resulted to the oxidation of the surface.After the samples was subjected to corrosion test, an increased layer of dense and non-uniform corrosion scales of 376.3 µm thickness was noticed. This shows that there is acceleration of corrosion of the substrate due to seawater and increased formation of corrosion scales as a result of oxidation reaction from sea water constituents. Plate 4 shows the HRSEM cross-section view of sample coated prior to corrosion test and after corrosion test.

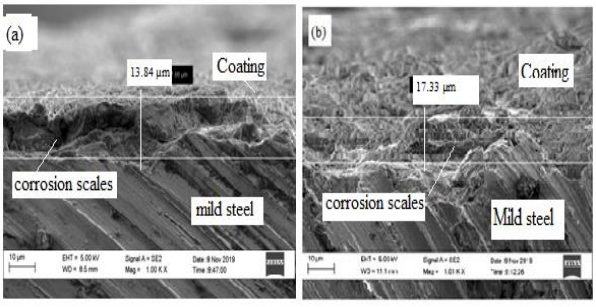

Plate 4: HRSEM cross-section view of coated sample (a) prior to corrosion test. (b) after corrosion test.

The cross-section view in Plate IV (a) shows a smoother layer of top coat with the corroded layer of 13.84 µm thickness as compared with the corrosion layer of 17.33 µm obtained after the specimen was subjected to corrosion test in seawater environment, as shown in plat IV (b). The result obtained from the SEM images shown in Plate IV is in agreement with the potentio-dynamic polarization Tafel plot which shows that the coated sample has the least negative potential hence, less susceptible to corrosion.

4 Conclusion

In this study the corrosion behaviour of Silver-Cobalt Oxide-Titanium Dioxode ($Ag/Co_3O_4/TiO_2$) nanocomposites coated mild steel in seawater environment was investigated. It was noticed that the coating on the specimen plays a key role to improve the resistance of mild steel to corrosion under sea water.

Acknowledgement

We wish to express our appreciation to the Centre for Genetic Engineering and Biotechnology, Federal University of Technology, Minna, for their assistance during sample analysis. We also appreciate the contribution following people who helped in the area of samples characterization which includes Dr Remy Bucher for XRD analysis at Ithemba Laboratory in South Africa, Dr. Franscious Cummings and Andrian Joseph for HRSEM, at Physics department, University of Western Cape in South Africa.

References

Abdulrahman, M.A., Abubakre, O.K., A bdalkereem., S.A., Tijani, J.O., Aliyu, A. and Afolabi, A.S. (2017): Effect of Coating Mild Steel with CNTS. On its Mechanical Properties and Corrosion Behavior in Acidic Medium. *Advances in Natural Science: Nanoscience and Nanotechnology 8. 015016 (14PP).*

Afolabi, A.S., and Muhirwa, A.C., Abdulkareem, A.S., and Muzenda, E, (2014): Weight Loss and Microstructural Studies of Stressed Mild Steel in Apple Juice. *International Journal of Electrochemical Science, (9) 5895-5906.*

ASTM-G59-97 (2009): Standard Test Methods for Conducting Potentiodynamic Polarization Resistance Measurement.

Attah, Y.A., El-Mahdy, G.A., Al-Lohedan, H.A and Ezzaat, A.O (2014): Synthesis and Application of Hybrid Polymer Composite Based on Silver Nanoparticles as Corrosion Protection for Line Pipe Steel. *Molcules (19): 6246-6262. Doi: 10.33990/molecules 19056246*

Bankole, M.T., Mohammed, I.A., Abdulkareem, A.S., Tijani, J.O., Ochigbo, S.S., Abukabre, O.K., Afolabi, A.S. (2018): Optimization of Supported Bimetallic (Fe-Co/$CaCo_3$) Catalyst Synthesis Parameters for Carbon Nanotubes Growth Using Factorial Experimental Design. *Journal of Alloys and compounds.*

Barchiche, C, Deslouis, C, Gil, O, Joiret, S, Refait, P, and Tribollet, B (2009): "Role of sulphate ions on the formation of calcareousdeposits on steel in artificial seawater; the formation of Green Rust compounds during cathodic protection," *ElectrochimicaActa*, 54(13) : 3580–3588

Behzadnasab,S. (2010): Corrosion Performance of Epoxy Coatings Containing Silane treated ZrO_2 Nanoparticles on Mild steel in 3.5% NaCl solution. Corrosion Science 53(1): 89-98. Doi:10.1016//j.corsci.2010.09.026

Fayomi, O.S.I and Popoola, A.P.I (2013): Anti-Corrosion Properties and Structural Characterization of Ternary Coating, ISSN 1068-3755. Surface Engineering and Applied Electrochemistry 51 (1) 76-84

Gadang P., Lutviasari N., Siska P., Sundjono, S, (2017): Corrosion Behavior of Mild Steel in seawater from Karangson and Eretan

of West Java region, Indonesia. *http://journal. Trunojoyo.ac.id/jurnal Kalautan 2(11). 1907-9931.*

Haijing, S., Weihai, X., Jiaxin, Xu, Guoliang, C., Jie, S. (2020): Cathodic Protection Criteria of Low Alloy Steel in Simulated Deep Water Environment, Anti -Corrosion Methods and Materials.

Karthick, S., Muralidharan, S., and Saraswathy, V. (2018): Corrosion Performance of Mild Steel and Galvanized Iron in Clay Soil Environment. *Arabian Journal of Chemistry,http://doi.org/10.1016/j,arabjc.11,005*

Malatji, N and Popoola, A.P.I, (2015): Electrodeposition of Ternary Zn-Cr O -SiO Nanocomposite Coating on Mild Steel for Extended Applications. *International Journal of Electrochemical science, (10) 3988-4003.*

Muhammad, F.M., Nazeri1., Shahadan M.S, Masri M.N., Nurhaswani, A., Abd Rashid, M.W., Yatimah A., and Mohamad, A. (2012): Corrosion and Heat Treatment of Paint Coating Containing Battery Cathode Waste Material-Epoxy Resin in 3.5 wt% Sodium Chloride Solution: *International Journal of Electrochemical Science (7); 9633 – 9642.*

Pineau, S., Sabot, R., Quillet, L (2008): Formation of the Fe (II-III) hydroxysulphate green rust during marine corrosion of Steel associated to molecular detection of dissimilatory sulphite-reductase. *Corrosion Science 50 (4); 1099-1111*

Refait, PH, Memet, J.B, Bon, C, Sabot, R, and G´enin, J.M.R (2003): "Formation of the Fe(II)–Fe(III) hydroxysulphate green rustduring marine corrosion of steel," *Corrosion Science*, 45(4) : 833–845

Sadeghimerisht, E., Markocsan, N. and Joshi, S. (2019): Advances in Corrosion-Resistant Thermal Spray Coatings for Renewable Power Plants. Part 1: Effect of Composition and Microstructure. *Journal of Thermal Spray Technology. 28, 1749-1788*

Seidu, S and Kutelu, B.J (2013): Effect of Heat treatments on Corrosion of Welded Low-Carbon Steel in Acid and Salt Environments. *Journal of Materials and Materials Characterization and Engineering 2 (3): 95-100 Doi: 10.4236/jmmc 13018.*

Somayeh, K., Bahram, G., and Reza, Y., (2018): The Effect of NanoParticle Coating on Anticorrosion Performance of Centrifugal Pump Blades. *Jordan Journal of Mechanical and Industrial Engineering 12(2): 117-122*ISSN 1995-6665

Srivastava, M (2006): Corrosion Resistance and Microstructure of Electrodeposite Nickel-Cobalt Alloys Coating. *Doi: 10.1016/j.surf. coating (6) 017*.

Subir, P. (2016): Corrosion Inhibition of Carbon Steel in Acidic Environment by Papaya Seed as Green Inhibitor. *Journal of Bio and Tribo corrosion 2(6).*

Umeozokwere, A.O, Mbabuike, I.U, Oreko, B.U and Ezemuo, D.T, (2016): Corrosion Rates and Impact on Mild Steel in some Selected Environment. Journal of Scientific and Engineering Research 3 (1) :34-43.

Umoru L.E (2001): Corrosion Study of AISI 304, AISI 321 and AISI 430 Stainless Steel in a Tar Sand Digester. Journal of Minerals and Materials Characterization and Engineering 7 (4): 291-299. Doi: 10.4236/jmmc 79022.